

Unusual glitch activity in the RRAT J1819–1458: an exhausted magnetar?

A. G. Lyne¹, M. A. McLaughlin^{2,3,4}, E. F. Keane¹, M. Kramer^{1,5}, C. M. Espinoza¹,
B. W. Stappers¹, N. T. Palliyaguru² & J. Miller²

¹ *Jodrell Bank Centre for Astrophysics, School of Physics and Astronomy, The University of Manchester, Manchester M13 9PL, UK*

² *Dept. of Physics, West Virginia University, Morgantown, WV 26506, USA*

³ *National Radio Astronomy Observatory, Green Bank, WV 24944, USA*

⁴ *Alfred P. Sloan Research Fellow*

⁵ *MPI für Radioastronomie, Auf dem Hügel 69, 53121 Bonn, Germany*

ABSTRACT

We present an analysis of regular timing observations of the high-magnetic-field Rotating Radio Transient (RRAT) J1819–1458 obtained using the 64-m Parkes and 76-m Lovell radio telescopes over the past five years. During this time, the RRAT has suffered two significant glitches with fractional frequency changes of 0.6×10^{-6} and 0.1×10^{-6} . Glitches of this magnitude are a phenomenon displayed by both radio pulsars and magnetars. However, the behaviour of J1819–1458 following these glitches is quite different to that which follows glitches in other neutron stars, since the glitch activity resulted in a significant long-term net decrease in the slow-down rate. If such glitches occur every 30 years, the spin-down rate, and by inference the magnetic dipole moment, will drop to zero on a timescale of a few thousand years. There are also significant increases in the rate of pulse detection and in the radio pulse energy immediately following the glitches.

Key words: pulsars: general

1 INTRODUCTION

Rotating Radio Transients (RRATs) are sporadic radio sources from which we detect bursts of emission of typically a few milliseconds duration and which occur at intervals of between a few minutes and a few hours. Eleven of these elusive objects were discovered in a single-pulse analysis of the Parkes Multibeam Pulsar Survey (McLaughlin et al. 2006), but they cannot be detected through their periodicity using standard Fourier or periodogram techniques. However, careful studies of the times of arrival of the bursts reveal underlying periodicities which indicate that they are rotating neutron stars. Since their discovery, a campaign of timing observations has been implemented in order to monitor the rotational history of these objects (McLaughlin et al. 2009). Rotating once every 4.26 seconds, J1819–1458 is the most prolific bursting RRAT. At 1.4 GHz it exhibits ~ 3 ms bursts with peak flux density as strong as ~ 10 Jy with a burst rate of $\sim 20 - 30 \text{ hr}^{-1}$. The high burst rate enabled a quick determination of a timing solution for this source and hence an accurate position. The true nature of this source as a neutron star was further illustrated by X-ray observations. These revealed a thermal X-ray spectrum which is what is

expected from a cooling neutron star (Reynolds et al. 2006; Gaensler et al. 2007; McLaughlin et al. 2007).

The discovery of RRATs raised interesting questions about the number of neutron stars in the Galaxy. Initial estimates indicate that RRATs may outnumber the normal radio pulsar population in the Galaxy by a factor of 4 (McLaughlin et al. 2006). It has been argued that the observed Galactic supernova rate seems now to be insufficient to account for the whole population of neutron stars (Keane & Kramer 2008), which include radio pulsars, millisecond pulsars, magnetars, RRATs, X-ray detected but radio quiet Isolated Neutron Stars (INSs) and the Central Compact Objects (CCOs), some of which are thought to be neutron stars. Evolution between the various populations of neutron stars could go some way towards resolving this problem. Indeed, there is evidence of an evolutionary trend connecting young pulsars with magnetars (Lyne 2004). Among the observed properties which suggest that the two populations may be linked are very low braking indices (Lyne et al. 1996), magnetar-like burst activity in one young pulsar (Kumar & Safi-Harb 2008; Gavriil et al. 2008), low luminosity during quiescence in var-

ious magnetars, resembling the X-ray emission of normal pulsars (Archibald et al. 2008), and pulsed magnetar radio emission (Camilo et al. 2006; Camilo et al. 2007).

Long-term timing of all these objects provides essential information needed to understand any evolutionary relationships between the different neutron star populations. Among the different trends and features observed in long-term data we find glitches, which are discontinuous events resulting in spin-up of the neutron star, and thought to be caused by the transfer of angular momentum from the rotating superfluid in the stellar interior to the outer crust. Glitches sometimes dominate the long-term spin evolution of pulsars (Lyne et al. 1996) and have been observed in numerous young pulsars and several magnetars, appearing to be a normal phenomenon among rotating neutron stars.

We describe the observations in section 2, before discussing the unusual glitch activity observed in RRAT J1819–1458 in section 3. In section 4 we discuss the implications of these results as they address to the relationship between RRATs and other neutron stars.

2 OBSERVATIONS

The observations reported here start with the discovery observation in August 1998, followed by an intensive 5-year series of recordings starting five years later. The measurements were carried out using the 64-m Parkes Telescope in Australia and the 76-m Lovell Telescope at Jodrell Bank in the United Kingdom at a frequency of 1.4 GHz. At Parkes, a dual-channel cryogenic receiver was used to receive orthogonal linear polarisations. Each channel was processed in a 512×0.5 -MHz filterbank, added in polarisation pairs to provide the total intensity, 1-bit sampled and recorded on tape. Observations at Parkes were typically 30 min in duration. At Jodrell Bank, a dual-channel cryogenic receiver was sensitive to the two hands of circular polarisation which were each processed in a 64×1 -MHz filterbank before being added to produce total intensity, 1-bit sampled and stored on tape. Observations at Jodrell Bank were 60 min in duration. The longer observations at Jodrell Bank were due to the lower sensitivity as a result of the narrower available bandwidth. We note also that the presence of broadband impulsive radio frequency interference hinders the identification of pulses from RRATs at both observatories. However, the quality of the observational data was markedly improved by the use of the zero-DM filtering algorithm (Eatough et al. 2009).

Off-line, the data were dedispersed at the nominal dispersion measure (DM) of the RRAT as well as at a number of adjacent DM values to aid RFI discrimination. The resulting time sequences were then searched for significant single bursts of radiation, whose times of arrival (TOAs) were recorded. We can compare the observed TOAs with a model of the neutron star’s rotational and astrometric parameters in a manner similar to standard pulsar timing (see Lorimer & Kramer (2005) or Lyne & Graham-Smith (2006)). The only difference is that standard pulsar methods obtain TOAs from integrated pulse profiles of as many as $10^2 - 10^4$ single pulses whereas for RRATs individual pulses have a sufficiently high S/N that we can obtain TOAs from individual pulses (and indeed are required to do so because of the sporadic emission). The differences between the observed

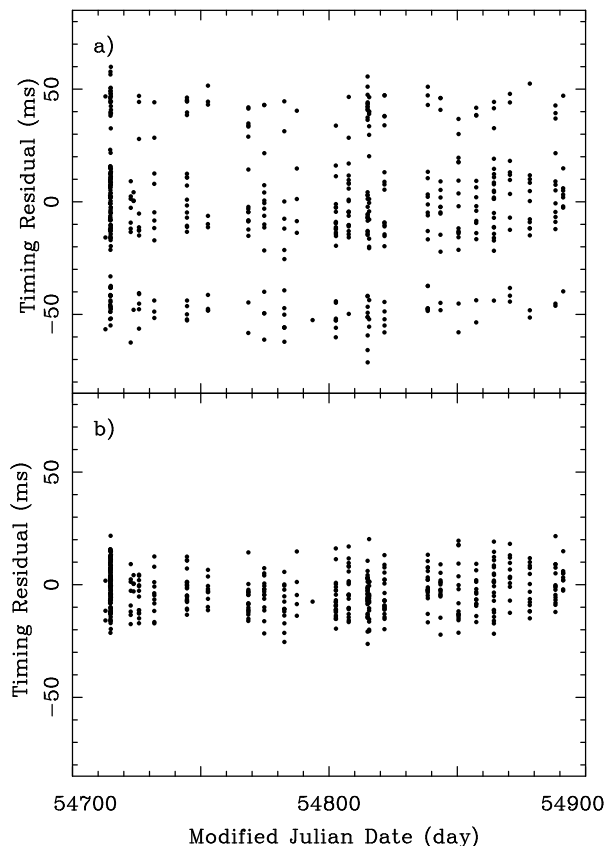


Figure 1. a) The timing residuals from the TOAs of the individual pulses from J1819–1458, relative to a simple slow-down model, showing that they are located in 3 clearly identifiable bands which are offset in pulse longitude by ± 45 ms. b) the same residuals, with the TOAs in the top band and the bottom band decreased and increased by 45 ms respectively. The rms of the residuals decreases from 21.2 ms to 9.1 ms.

arrival times and the predicted arrival times are known as the pulsar’s “timing residuals” and the model parameters (such as period, period derivative and sky position) are determined by adjusting their values to minimise the rms value of the residuals.

3 RESULTS

Tri-Modal Residuals

In Fig. 1, we plot the timing residuals for all the bursts received from J1819–1458 over the most recent 200 days relative to a simple slow-down model which includes only the spin frequency and its first derivative. The upper plot shows that the bursts from J1819–1458 arrive over a longitude range spanning approximately 120 ms and grouped within three longitude regions separated by about 45 ms.

Fortunately, within a single 30-min or 60-min observation there is a sufficiently large number of bursts to allow each burst to be uniquely identified with one of the three

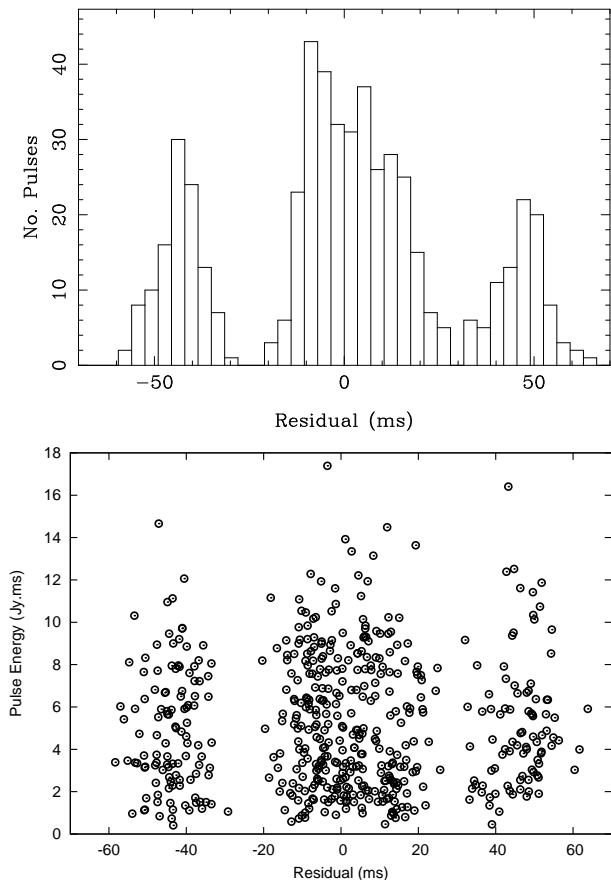


Figure 2. Top: Distribution of the timing residuals of bursts from RRAT J1819–1458 where the three bands seen in Fig. 1a are clear. Bottom: A scatter plot of pulse energy versus timing residual.

bands. Those TOAs identified with the upper and lower bands are either decreased by 45 ms or increased by 45 ms respectively and the residuals recalculated. The lower diagram in Fig. 1 shows the residuals resulting from this recalculation. As a result of this procedure the rms value of the residuals is reduced by a factor of ~ 2.5 and the uncertainties in the fitted parameters are similarly reduced. The timing analyses presented in this paper are based upon all the TOAs modified in this fashion.

Most of the bursts ($\sim 60\%$) come from the middle band, where also the brightest bursts are found. The top panel of Fig. 2 shows a collapsed histogram of the timing residuals of the top panel of Fig. 1. This is essentially a probability distribution in rotational phase for the bursts. The three-band structure is consistent with the three-component profile reported by Karastergiou et al. (2009). In Fig. 3, we show a sequence of pulses detected during a single long Parkes observation, along with the composite profile formed by summing all of these individual pulses, which show anywhere from one to four components. Such composite profiles vary from day to day due to the large degree of pulse-to-pulse variation.

Esamdin et al. (2008) reported the presence of only two preferred longitude ranges, using the 25-m radio telescope at Urumqi. However, because of the smaller size of that telescope, they were only sensitive to the most intense bursts,

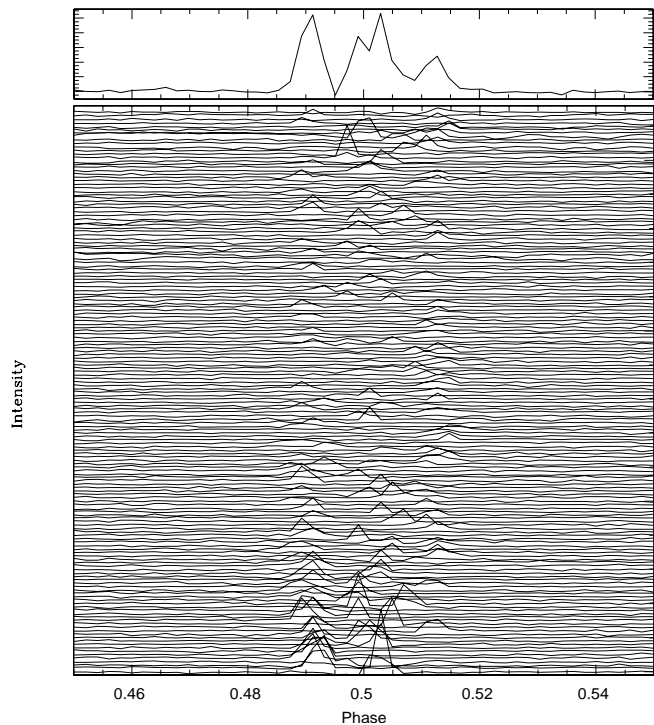


Figure 3. All 165 single pulses detected during an eight-hr observation of J1819–1458 with Parkes at 1.4 GHz (bottom) along with the composite profile formed by summing all 165 pulses (top). The time intervals between the pulses vary.

those having flux densities $\gtrsim 3.4$ Jy, resulting in the observation of only 162 bursts in 94 hours of observation, or a burst rate of 1.7 hr^{-1} . Most of the bursts came from the middle band, with 18 from the early band and just 2 from the later band. The higher sensitivity of the larger telescopes used in the present experiment allowed us to detect $\gtrsim 500$ bursts from RRAT J1819–1458 in 27 hours of observation at rates of $\sim 15 - 20 \text{ hr}^{-1}$ at Jodrell Bank, and somewhat higher at Parkes. The bottom panel of Fig. 2 shows the intensity distributions of bursts in the three bands. In determining pulse intensities, we used the sky temperature model of Haslam et al. (1982) extrapolated from 430-MHz to 1400-MHz assuming a spectral index of -2.6 (Lawson et al. 1987). Taking into account the higher flux density limit of the Urumqi observations and the unknown amplitude distribution within the bands at high flux density, the two sets of results appear consistent.

The three-component profile is consistent with the trimodal timing residuals, and can be reconciled with a patchy emission beam with core and conal components (e.g. Lyne & Manchester 1988). We expect that many normal pulsars with profiles with multiple components would exhibit similar bi- or tri-modal residuals if timed through their single pulses.

Glitches

Fig. 4a shows the evolution of the rotational frequency over a ~ 10 -yr interval. In the upper diagram, the steady slow-down is interrupted at around MJD 53900 by a sudden spin-up. The nature of this spin-up can be seen more clearly in Fig. 4b, which displays the frequency residuals relative

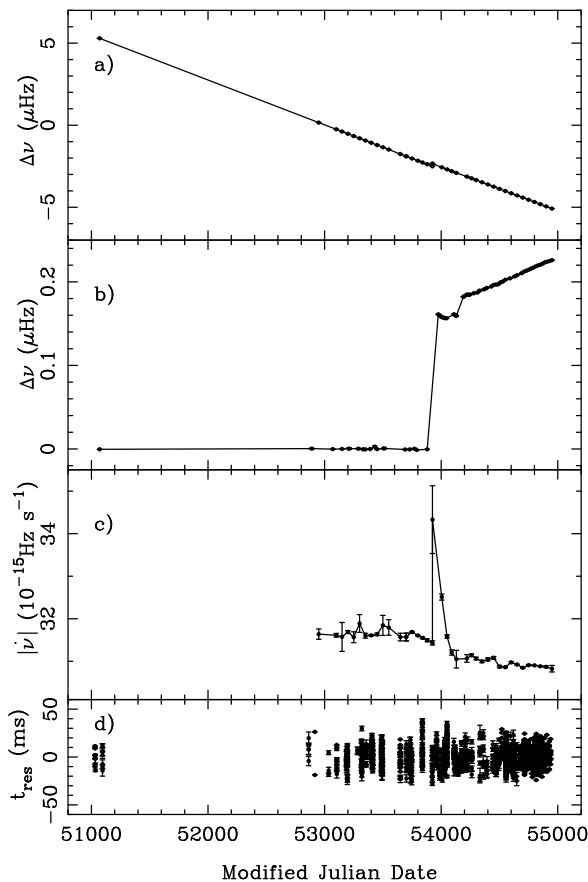


Figure 4. The frequency evolution of the RRAT J1819–1458 over a 10-year period. a) shows the secular slowdown in rotation rate of the neutron star, interrupted by a major glitch which is seen as a clear discontinuity at around MJD 53900. b) shows the frequency residuals relative to a simple slow-down model fitted to data between MJD 51000 and 53900 and reveals the presence of a second, smaller glitch, about 200 days later. c) presents the variation in the magnitude of frequency derivative $|\dot{\nu}|$, showing a significant decrease in the rate of slowdown following the glitches. d) shows the timing residuals t_{res} relative to the rotational model given in Table 1.

to a simple slow-down model fitted to the TOAs obtained prior to MJD 53925. The spin-up is revealed as being due to two glitches, quite close to one another, occurring at around MJD 53926 and MJD 54167, followed by a period of steadily increasing frequency relative to the model. The latter corresponds to a reduced magnitude of frequency first derivative, which can be seen in Fig. 4c following a transient short-term increase.

In order to quantify these changes, the TEMPO¹ pulsar timing package was used to model the slowdown of the pulsar and the two glitches. It was found necessary to include steps in both ν and $\dot{\nu}$ and a decaying exponential for the first glitch but only a step in ν for the much smaller second glitch. These parameters are given in Table 1. For this timing analysis,

¹ <http://pulsar.princeton.edu/tempo>

Table 1. The observed and derived rotational parameters of the RRAT J1819–1458.

Timing parameters	
Right Ascension α	$18^{\text{h}}19^{\text{m}}34^{\text{s}}.173$
Declination δ	$-14^{\circ}58'03''.57$
Frequency ν (Hz)	$0.23456756350(2)$
Frequency derivative $\dot{\nu}$ (s^{-2})	$-31.647(1) \times 10^{-15}$
Timing Epoch (MJD)	54451.0
Dispersion measure DM (cm^{-3}pc)	196
Timing data span (MJD)	51031 – 54938
RMS timing residual σ (msec)	10.2
Glitch 1 Parameters	
Epoch (MJD)	53924.79(15)
Incremental $\Delta\nu$ (Hz)	$0.1380(6) \times 10^{-6}$
Incremental $\Delta\dot{\nu}$ (s^{-2})	$0.789(6) \times 10^{-15}$
Decay $\delta\nu$ (Hz)	$0.0260(8) \times 10^{-6}$
Decay timescale τ (days)	167(6)
Glitch 2 Parameters	
Epoch (MJD)	54168.6(8)
Incremental $\Delta\nu$ (Hz)	$0.0226(3) \times 10^{-6}$
Derived Parameters	
Characteristic Age (kyr)	120
Surface Magnetic Field (G)	50×10^{12}

we used the position of J1819–1458 derived from Chandra X-ray observations of the source (Rea et al. 2009), which has errors of 0.2 arcsec in both coordinates. The value of dispersion measure used was that given by McLaughlin et al. (2006).

Glitches usually display fractional increases in rotational frequency $\Delta\nu/\nu$ which range between 10^{-9} and 10^{-5} (e.g. Lyne, Shemar & Graham-Smith 2000). The two glitches in J1819–1458 have $\Delta\nu/\nu = 0.6 \times 10^{-6}$ and 0.1×10^{-6} . While these are not the largest glitches known (c.f. Hobbs et al. 2002) they are typical in fractional size to those from many young pulsars (e.g. Zou et al. 2008) and magnetars (Mereghetti 2008).

Glitch-associated emission activity

In Fig. 5, we show the rate of pulse detection (top) and the peak pulse energy (bottom) for each observation as a function of date for J1819–1458. For both quantities, there is a large variation, with maximum values in the observation (on MJD 53960) which immediately follows the first, and largest, glitch. On this date, the mean pulse detection rate is 68 ± 12 pulses/hour, 2.8 times the mean and significant at the 3.5σ level. The corresponding value of the peak pulse energy is 58.7 mJy.s, which is 3.7 times the mean and significant at the 4.7σ level. We note, however, that the high burst rate on MJD 54619 is not associated with any obvious timing abnormality.

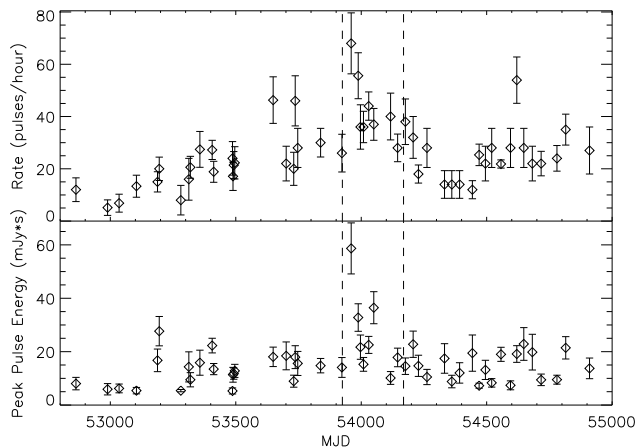


Figure 5. The variation of rate of pulse detection (top) and the peak pulse energy (bottom) with date for J1819–1458. The epochs of the two glitches are marked with dashed lines. As a control experiment, we find no dependence of the pulse detection rate on varying sensitivity due to the zenith angle of the observations.

4 DISCUSSION

While J1819–1458 exhibits many of the properties of normal, relatively young radio pulsars, namely rapid spin-down and glitches, the behaviour following the glitch activity is quite different. The main effect is a long-term reduction in the magnitude of the slow-down rate. This is unlike all observed glitches in radio pulsars and magnetars, which always lead to a long-term increase in the rate of slow-down. Fig. 6 illustrates this by showing the behaviour of slow-down rate for J1819–1458 and a selection of normal young pulsars for a few hundred days around typical glitches. The behaviour of the Crab pulsar (B0531+21) shows the greatest similarity to that of J1819–1458, each displaying a relatively short-term transient before reaching a new asymptotic slow-down rate, although the long-term net increments in slow-down rate clearly have different signs.

Fig. 7 shows the $P-\dot{P}$ diagram for normal pulsars, magnetars and other RRATs (McLaughlin et al. 2009). Objects with constant dipolar magnetic field move towards the lower right-hand corner of the diagram with a slope of -1 . Young normal pulsars are observed to move with a slope of between -1.0 and $+0.5$. On this diagram, glitches from normal pulsars such as those shown in Fig. 6 result in a net increase in slow-down rate and an upwards step in the $P-\dot{P}$ diagram. On the other hand, RRAT J1819–1458 stepped vertically downwards, towards smaller values of \dot{P} . If this particular post-glitch behaviour is typical, then the long-term effect of any glitches would be a secular movement towards the bottom of the $P-\dot{P}$ diagram. If such glitches were to occur every 30 years, then the slowdown rate would decay to zero on a timescale of only a few thousand years. Only larger timespan observations will unveil the actual path of RRATs on the $P-\dot{P}$ diagram. If the trend continues it could indicate that the RRAT started off in the region of the diagram populated by the magnetars.

Glitches are understood to be caused by the communication between a superfluid component of the neutron star interior and the crust. In the standard model, a neutron star

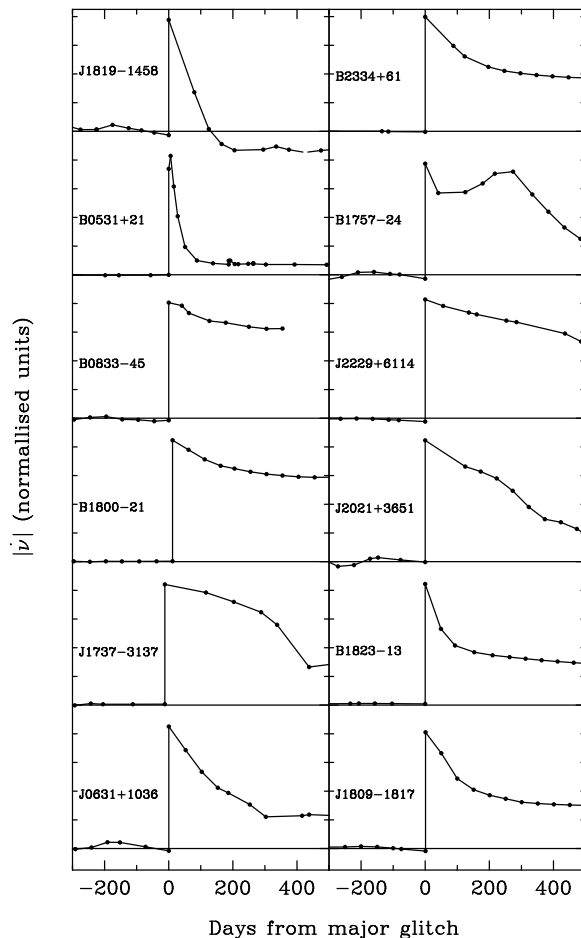


Figure 6. The changes in the magnitude of the first derivative of the rotational frequency $|\dot{\nu}|$ near the glitch from the RRAT J1819–1458 and near typical glitches in 11 pulsars. A second frequency derivative has been fitted to each pre-glitch data set and subtracted from the whole set. The scale of each diagram has been adjusted so that the step change in value at the glitch is the same. Without exception, the final values of $|\dot{\nu}|$ for the pulsars are greater than before the glitches. In the case of J1819–1458, there is a net decrease in magnitude.

has a superfluid that is originally spinning faster than the crust (see, e.g. Anderson & Itoh 1975, Alpar & Pines 1993). This is because the magnetic dipole acts on the crust and the coupled core, with the crustal superfluid rotating independently. All neutron stars, regardless of their observational manifestation, are expected to show this same structure. The angular momentum resides on vortex lines, which are pinned to nuclei in the crust. These lines suffer strong forces due to the mismatch between the superfluid and crustal velocities. A glitch occurs when there is a sudden unpinning of the vortex lines, and subsequent transfer of angular momentum from the superfluid to the crust. In a magnetar, glitches could occur due to the high internal magnetic field that can deform or crack the crust (Thompson & Duncan 1996).

It could be that the strange glitch behavior of J1819–1458 is due to a different mechanism for the unpinning, namely the deformation or cracking of the crust due to the high magnetic field, as opposed to the unpin-

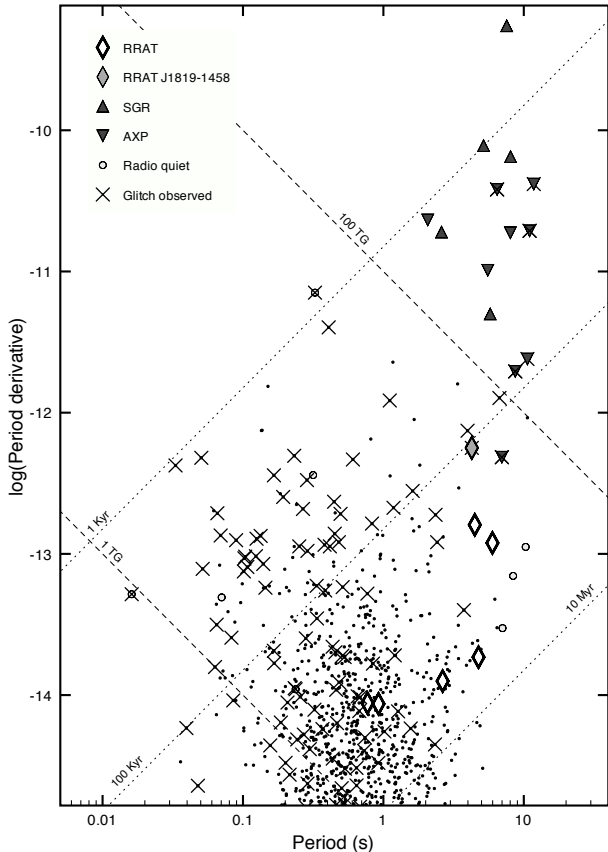


Figure 7. The $P-\dot{P}$ diagram for normal young pulsars and magnetars, as well as for the RRAT J1819–1458 (filled diamond) and other RRATs (open diamonds).

ning due to the angular velocity lag as suggested for normal pulsar glitches. While a magnetar glitch which resulted in a decrease in the spin-down rate has not yet been observed, magnetar glitches seem to show different characteristics to radio pulsar glitches. Gavriil et al. (2009) showed that AXP 4U 0142+61 suffered a glitch that resulted in a net spin-down. They interpret this as being due to some regions of the superfluid originally spinning slower than the crust, as opposed to faster in normal rotation-powered pulsars.

Magnetar glitches are occasionally associated with radiative events and pulse profile and spectral changes (see, e.g. Dib et al. 2008), with no obvious relationship between the size of the glitch and the extent of these changes. The increase in both burst rate and peak pulse energy immediately following the first glitch in J1819–1458 is suggestive of an association. Both these quantities seem to be sustained at a raised level for 100–200 days. Although there are some days with nearly as high a burst rate that are not associated with any timing irregularity, the fact that both burst rate and pulse energy are associated with the glitch suggests that this is not just a statistical fluke. More large glitches must be detected for such correlations to be tested robustly. In addition, X-ray observations immediately after the next large glitch would be useful to search for magnetar-like bursts or correlated pulse profile or spectral changes.

5 CONCLUSION

In this paper, we have demonstrated the difficulty of timing pulsars with multiple components through their single pulses, and have presented a simple algorithm for mitigating these effects.

We have presented a timing analysis of the RRAT J1819–1458 over the past 5 yr and report the detection of two significant glitches. The magnitudes of these glitches are similar to those measured for radio pulsars and magnetars, but the behaviour after the glitch is quite different. The glitches have resulted in a long-term net decrease in the slow-down rate, corresponding to a downward vertical movement on the $P-\dot{P}$ diagram. This jump in frequency derivative is $\sim 0.75(5) \times 10^{-15} \text{ Hz s}^{-1}$, corresponding to a $\sim 1\%$ decrease of the surface magnetic field of the neutron star. If such glitches are representative behaviour of this RRAT and were to occur every 30 years, the spin-down rate, and by inference the magnetic dipole moment, will drop to zero on a timescale of a few thousand years. This implies that J1819–1458 may have begun its life in the magnetar region of the diagram.

We have also briefly discussed the evolution of the burst rate and peak flux density of pulses from J1819–1458 with time, and showed that both peaked immediately after the large glitch. This is tantalizing evidence for a similarity with magnetar glitches.

ACKNOWLEDGEMENTS

We thank all the pulsar observers at Parkes for assistance with these observations. MAM and NTP are supported by a WV EPSCOR grant. EK acknowledges the support of a Marie-Curie EST Fellowship with the FP6 Network “ESTRELA” under contract number MEST-CT-2005-19669. CME thanks the support received from STFC and CONICYT through the PPARC-Gemini fellowship PPA/S/G/2006/04449.

REFERENCES

- Alpar M. A., Pines D., 1993, in K. A. van Riper R. E., Ho C., eds, *Isolated Pulsars*. Cambridge University Press, p. 17
- Anderson P. W., Itoh N., 1975, *Nature*, 256, 25
- Archibald A. M., Kaspi V. M., Livingstone M. A., McLaughlin M. A., 2008, *ApJ*, 688, 550
- Camilo F., Ransom S. M., Halpern J. P., Reynolds J., Helfand D. J., Zimmerman N., Sarkissian J., 2006, *Nature*, 442, 892
- Camilo F., Ransom S. M., Halpern J. P., Reynolds J., 2007, *ApJ*, 666, L93
- Dib R., Kaspi V. M., Gavriil F. P., 2008, *ArXiv e-prints* (0811.2659)
- Eatough R. P., Keane E. F., Lyne A. G., 2009, *MNRAS*, 395, 410
- Esamdin A., Zhao C. S., Yan Y., Wang N., Nizamidin H., Liu Z. Y., 2008, *MNRAS*, 389, 1399
- Gaensler B. M. et al., 2007, *apss*, 308, 95
- Gavriil F. P., Dib R., Kaspi V. M., 2009, *ArXiv e-prints*
- Gavriil F. P., Gonzalez M. E., Gotthelf E. V., Kaspi V. M., Livingstone M. A., Woods P. M., 2008, *Science*, 319, 1802
- Haslam C. G. T., Stoffel H., Salter C. J., Wilson W. E., 1982, *A&AS*, 47, 1
- Hobbs G. et al., 2002, *MNRAS*, 333, L7

- Karastergiou A., Hotan A. W., van Straten W., McLaughlin M. A., Ord S. M., 2009, *MNRAS*, 396, L95
- Keane E. F., Kramer M., 2008, *MNRAS*, 391, 2009
- Kumar H. S., Safi-Harb S., 2008, *ApJ*, 678, L43
- Lawson K. D., Mayer C. J., Osborne J. L., Parkinson M. L., 1987, *MNRAS*, 225, 307
- Lorimer D. R., Kramer M., 2005, *Handbook of Pulsar Astronomy*. Cambridge University Press
- Lyne A. G., Manchester R. N., 1988, *MNRAS*, 234, 477
- Lyne A. G., Smith F. G., 2006, *Pulsar Astronomy*, 3rd ed. Cambridge University Press, Cambridge
- Lyne A. G., 2004, in Camilo F., Gaensler B. M., eds, *Young Neutron Stars and Their Environments*, IAU Symposium 218. Astronomical Society of the Pacific, San Francisco, p. 257
- Lyne A. G., Pritchard R. S., Graham-Smith F., Camilo F., 1996, *Nature*, 381, 497
- Lyne A. G., Shemar S. L., Graham-Smith F., 2000, *MNRAS*, 315, 534
- McLaughlin M. A. et al., 2006, *Nature*, 439, 817
- McLaughlin M. A. et al., 2007, *ApJ*, 670, 1307
- McLaughlin M. A., Lyne A. G., Keane E. F., Kramer M., Miller J., Lorimer D. R., Manchester R. N., 2009, *MNRAS*, submitted
- Mereghetti S., 2008, *Astron. Astrophys. Rev.*, 15, 225
- Press W. H., Flannery B. P., Teukolsky S. A., Vetterling W. T., 1986, *Numerical Recipes: The Art of Scientific Computing*. Cambridge University Press, Cambridge
- Reynolds S. et al., 2006, *ApJ*, 639, L71
- Thompson C., Duncan R. C., 1996, *ApJ*, 473, 322
- Zou W. Z., Wang N., Manchester R. N., Urama J. O., Hobbs G., Liu Z. Y., Yuan J. P., 2008, *MNRAS*, 384, 1063